THE ARCHIVE OF MECHANICAL ENGINEERING

VOL. LIV 2007 Number 4

DOI: 10.24425/ame.2007.131562

Key words: electrodynamic forming, inductors

JÓZEF BEDNARCZYK *

STRESS AND DEFORMATION STATES IN SINGLE-COIL INDUCTORS USED FOR PIPE CALIBRATION BY MEANS OF ELECTRODYNAMIC METHOD

The article presents results of tests performed at the AGH-University of Science and Technology in Cracow on strength of single-coil inductors used as tools in electrodynamic machining of pipes. The character of volumetric Lorentz forces acting on coils of compressing and expanding inductors was discussed, and numerically determined distributions of stresses and displacements created in coils under the impact of these forces were presented. The problems presented are relevant when designing durable inductors intended for industrial applications.

1. Introduction

Electrodynamic method (ED) is unconventional technology of plastic forming of metals, in which one uses volumetric Lorentz forces generated in impulse magnetic field. In the case of electrodynamic forming of pipes, an electric coil – inductor – of specific length is slid over or inserted into a pipe with a tool. Forming of pipe ends on a short section is done using inductors in the form of a single coil, which can be oriented against the pipe as shown in Fig 1. The terminals of inductor 1 connected with output terminals of the generator deliver current defined by the following function:

$$i(t) = i_m e^{-\alpha t} \sin \omega t \tag{1}$$

where:
$\alpha = \dfrac{R}{2L}$ – coefficient of current suppression in discharge circuit; R, L – circuit resistance and inductance, respectively,

* *Department of Process Control, AGH-University of Science and Technology, Cracow, al. Mickiewicza 30, Poland; E-mail: bednarcz@agh.edu.pl*

$\omega = \sqrt{\frac{1}{LC} - \left(\frac{R}{2L}\right)^2}$ – angular frequency of damped vibrations for discharge current time function.

Current (1) is generated as a result of oscillatory discharge in time t of condenser 3 of capacitance C, which is the generator component, [2]. Short-time current i flowing through inductor coil 1 induces alternating magnetic field around it, which in turn induces eddy current I in the pipe wall. The flow of currents marked in Fig. 1 generates Lorentz force, which expands (Fig. 1a) or compresses (Fig. 1b) the pipe end. The expansion effect in practice is used, among other things, to make sockets or flanges formed using a die, (Fig. 2), and electrodynamic compression is used in assembly operations, (Fig. 3), [2]. Lorentz force, which loads the coil on a reaction basis, may have destructive effect resulting in deformation or permanent damage to the inductor head.

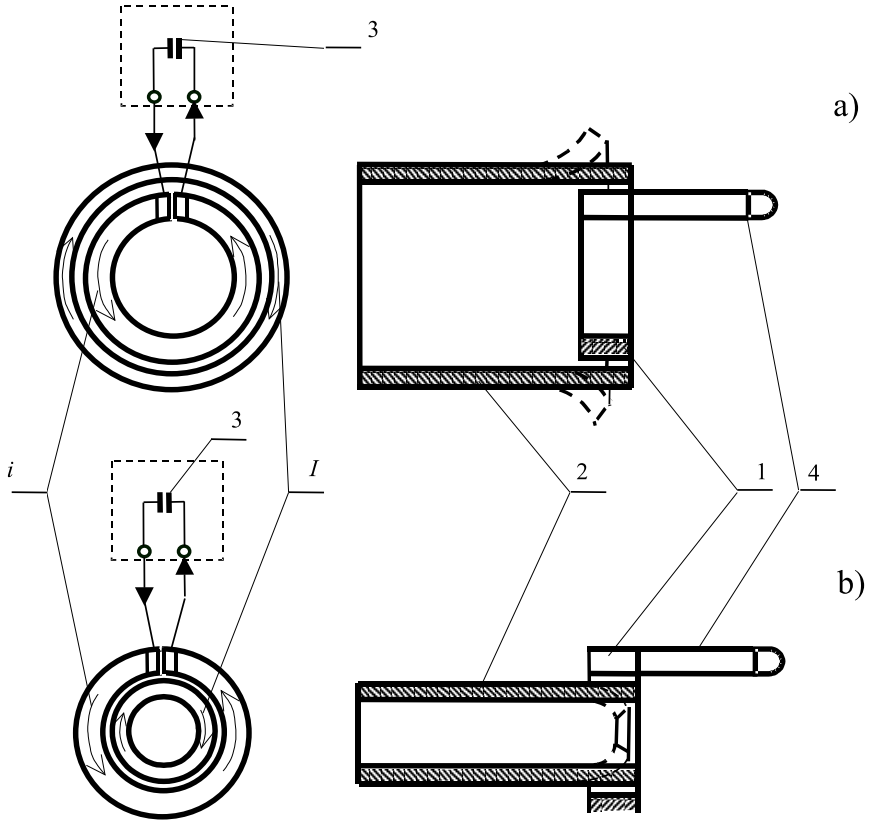

Fig. 1. Diagram showing pipe end electrodynamic forming using a single-coil inductor; (a) expansion, (b) compression: 1 – inductor, 2 – pipe, 3 – capacitor, 4 – inductor leads, i – capacitor discharge current, I – current induced in pipe wall

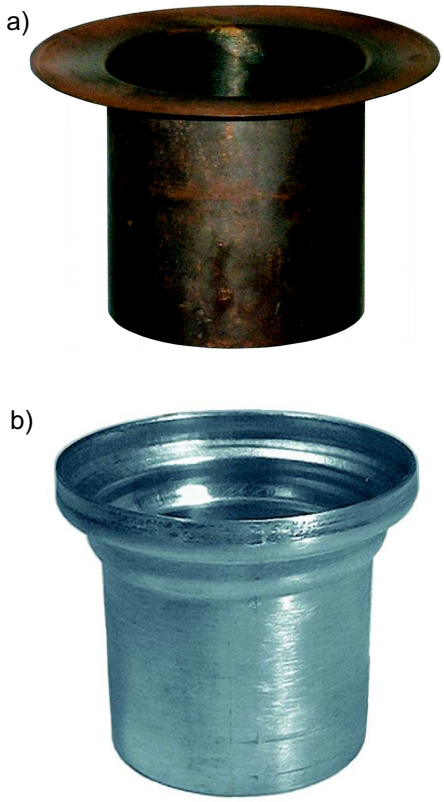

Fig. 2. Electrodynamic forming of flange (a) and socket (b) at pipe end using expanding inductor

Fig. 3. Fitting of an aluminum drive shaft using the electrodynamic method

Considering the state of technology presented in literature [5], [7], [8], [13], [15], [16] one can conclude that most of publications concerning the ED method are informative, and they describe possible applications of the method in practice. On the other hand, there are few publications, including [4], [9], [17], which cover the design and operation of instruments, e.g. inductors, used as machining tools in the ED technology. Obviously, implementing the electrodynamic method on an industrial scale is reasonable when inductor heads of high durability, which can be used many times in the production process, are available.

The article presents the results of analytical tests conducted at the AGH-University of Science and Technology in Cracow regarding the character of Lorentz forces and distribution of mechanical stress and deformation produced in single-coil inductors under these forces during electrodynamic machining of pipes [1], [2], [3], [10]. These issues are important when designing inductor heads, meeting construction safety and rigidity requirements while avoiding resizing the designed head elements.

2. Character of forces generated in single-coil inductors

The force $\mathrm{d}\overline{F}$ acting on an elementary volume $\mathrm{d}V$ of conductor conducting electric current i with density $\overline{j}$ placed in magnetic field with induction $\overline{B}$, is defined by the following equation [11]:

$$\mathrm{d}\overline{F} = (\overline{j} \times \overline{B})\mathrm{d}V = \overline{f}\mathrm{d}V \tag{2}$$

where vector product denotes density of Lorentz force $\overline{f}$.

The value of force defined by equation (2) depends on the value of induction B for resultant magnetic field generated by the following currents: i flowing in inductor coil and eddy current I induced in pipe wall, whereas the force direction results from spatial location of vectors $\overline{j}$ and $\overline{B}$.

In order to determine the nature of Lorentz forces acting on particles of the inductor conductor conducting current i in the absence of the processed pipe, the cylindrical coordinates r, φ, z are used for description of the circularly-placed coil, following the convention that inductor axis coincides with axis z of the said coordinate system, and coil is oriented in the plane parallel to plane (φ, r) of this system. With the assumption, satisfied in practice, that the length of the coil along axis z is considerably lower than its dimensions in plane (φ, r), density of current flowing in the coil has circumferential component j_φ only, and axial component B_{iz} is dominant in the magnetic field generated by this current.

This effect results from equipotentiality of coil plane [11], which means that induction of the vector is perpendicular to this plane in its every point Therefore, for the described conditions, the following dependencies are valid:

$$j_z = 0, \quad j_r = 0, \quad j_\varphi \neq 0 \tag{3}$$

$$B_{ir} = 0, \quad B_{i\varphi} = 0, \quad B_{iz} \neq 0 \tag{4}$$

By developing rotation in equation (2) considering relations (3) and (4) one derives the following formula

$$f_r = \overline{1}_r j_\varphi B_{iz} \tag{5}$$

Interpretation of formula (5) leads to the conclusion that current flow in circularly-bent inductor coil induces Lorentz forces acting on its particles in radial direction, and when current density is known, force values are determined by axial component of magnetic field induction B_{iz}, generated by the above-mentioned current.

If we place metallic pipe inside or outside the inductor carrying current of density $\overline{j}$, then variable magnetic field generated around it of intensity $\overline{H}_i$ defined by equation (6) penetrates into the pipe wall and induces electric field of intensity $\overline{E}$, equation (7). It is a source of rotary current I generated in the pipe, whose density is determined by equation (9). Equation (8) defines relation between intensity H and induction B in analysed magnetic field, (μ – magnetic permeability).

$$\mathrm{rot}\overline{H_i} = \overline{j} \tag{6}$$

$$\mathrm{rot}\overline{E} = -\frac{\partial \overline{B_i}}{\partial t} \tag{7}$$

$$\overline{B} = \mu \overline{H} \tag{8}$$

$$\overline{J} = \gamma \overline{E} \tag{9}$$

(γ – electrical conductivity).

When we compare equation (6) to equation

$$rot\overline{J} = -\mu\gamma \frac{\partial \overline{H_i}}{\partial t} \tag{10}$$

obtained by substituting (9) and (8) into equation (7), we can prove that the senses of currents in the inductor and the pipe wall are opposite, which is

the reason for mutual repulsion of the inductor coils and pipe wall during working. By expanding the rotation in equation (7) in cylindrical coordinates for conditions of axial symmetry in the inductor-pipe arrangement, and taking into account conditions (4) and relations (8) and (9), we derive the following relation

$$\frac{\partial(rJ_\varphi)}{r\partial r} = -\gamma\mu\frac{\partial H_{i\,z}}{\partial t} \tag{11}$$

which proves that density vector of rotary current in pipe wall has only circumferential component

$$J_\varphi \neq 0, \quad J_z = J_r = 0 \tag{12}$$

The analysis of electromagnetic field performed on the grounds of rotation expansion in equation (13)

$$\mathrm{rot}\overline{H_r} = \overline{J} \tag{13}$$

assuming that conditions (12) are satisfied and circumference symmetry of eddy current in pipe wall is taken into account, leads to the conclusion that axial component predominates in magnetic field generated by rotary current, similarly as in the magnetic field induced by current flow in inductor coil. Recapitulating the presented considerations, we can state that, at a specific moment of time, the forces generated by the resultant magnetic field act upon each inductor coil element that conducts current i. This magnetic field is produced by the forced current in the inductor coil and the eddy current induced in pipe, whereas eddy current I flows in pipe wall along the lines that form concentric circles whose centres lie within the inductor axis z. Density vectors for these currents, in which circumferential components j_φ, and J_φ predominate, have opposite senses, which determines the sense of the produced Lorentz force (pipe and coil repulsion). The resultant magnetic field generated by the above-mentioned currents has only axial component B_{wz}, resulting in radial direction of the Lorentz force. Therefore, the problem of determination, using formula (2), of the force acting upon a selected inductor coil element, which conducts current of known density, can be reduced to computing axial component B_{wz} of induction of the resultant magnetic field.

Density distribution of oscillatory current flowing in the inductor coil is determined by its thickness and current angular frequency ω. The inductor (Fig. 4) can be coiled using a conductor of relatively small thickness $g = a_2 - a_1$, or it can also be made in a form of a solid Bitter disk, in which $a_2 >> a_1$. The dimension $2b$ of the coil is equal to the length of the section along the pipe axis, on which pipe is to be formed. One of the premises for

selecting coil thickness is the condition to concentrate the current in the part where the processed semi-product is placed, [10]. This allows us to generate magnetic field in the inductor-semi-product configuration, and the field will be the source of a high-value Lorentz force acting on the semi-product. Alternating current evokes skin effect, in the metal coil of conductivity γ, so that the width of the current stream is not much greater than the skin depth $\delta = \sqrt{\frac{2}{\omega\mu\gamma}}$. The following relations between coil thickness – g and skin depth – determine distribution of current density in the inductor.

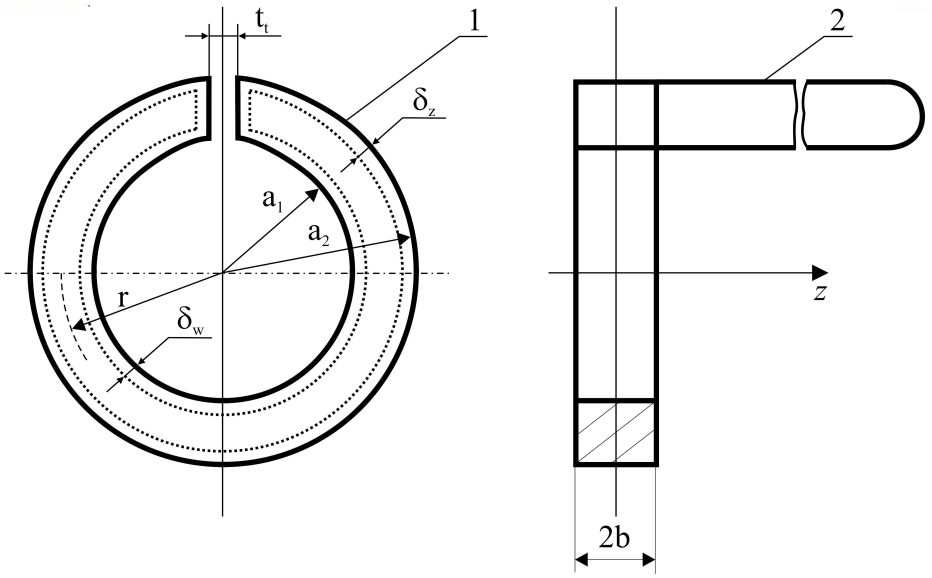

Fig. 4. Single-coil inductor: 1 – inductor coil, 2 – inductor end; δ_z, δ_w widths of outer and inner skin layers

For small value of ω the inequality $g < \delta$ is satisfied, then skin effect can be omitted, and distribution of current density flowing in inductor coil depends only on its thickness. In the conductor of small cross-section area, current density is constant. However, current density in the cross-section of a thick coil made in a form of Bitter disk varies according to formula [11]

$$j = j_w \frac{a_1}{r} \tag{14}$$

where j_w is current density on the coil internal surface if $r = a_1$.
For high value of angular frequency ω the inequality $g > \delta$ is satisfied, then skin effect is clearly evident, and it causes that the current flows in the coil only in the skin layers: δ_z and δ_w located near outer and inner coil surfaces,

Fig. 4. Current intensity in the said skin layers is inversely proportional to the inductance of these layers: L_z and L_w, the values of which are in turn directly proportional to radiuses of the layers [11].

3. The method used to compute Lorentz forces

The principle of superposition for magnetic field induction components generated in a certain area of inductor by currents flowing in the coil and in the semi-finished product was used to compute the values of forces acting on the coil element dV placed in that area. The computations were performed using relation (2), for known current density distribution in coil cross-section. This computation method allows determining force value very precisely [14]. The inductor was treated as a system of elementary circular coils with negligibly small cross-section, and the layer conducting eddy current in the semi-finished product was replaced by elementary current streams. For computations, we used equation (15) specified in [3], [11], which determines axial component of magnetic field induction at point $P(r_P,\ z_P)$ in space, where magnetic field is induced by current flowing in infinitely thin coil of radius a.

$$B_{Pw\,z} = \frac{\mu_0 i}{2\pi}\left[(a+r_P)^2 + z_P^2\right]^{-0,5}\left[\mathrm{K}(k) + \frac{a^2 - r_P^2 - z_P^2}{(a-r_P)^2 + z_P^2}\mathrm{E}(k)\right] \tag{15}$$

where: K, E – absolute elliptic integrals of first and second type, respectively

$$k_P = \left[\frac{4ar_P}{(a+r_P)^2 + z_P^2}\right]^{0,5}$$

Distributions of volumetric forces acting on inductor coil molecules without semi-finished product and at various inductor-pipe configurations were determined using numerical methods, by means of an original application developed using the C^{++} programming language. The created algorithm for computing forces in a certain inductor coil area was based on the principle of superposition for force reactions from elementary coils with current, using formula (2) and equation (15), in which $z_P = 0$, because the condition that coil dimensions along axis z are much smaller than those in the plane (φ, r) was satisfied. Only current layers of thickness δ were taken into account while determining distributions of Lorentz forces in coils clearly showing the skin effect.

For inductors selected as an example, Figs. 5 and 6 show the determined distributions of Lorentz forces along the radius, first in a thin inductor coil,

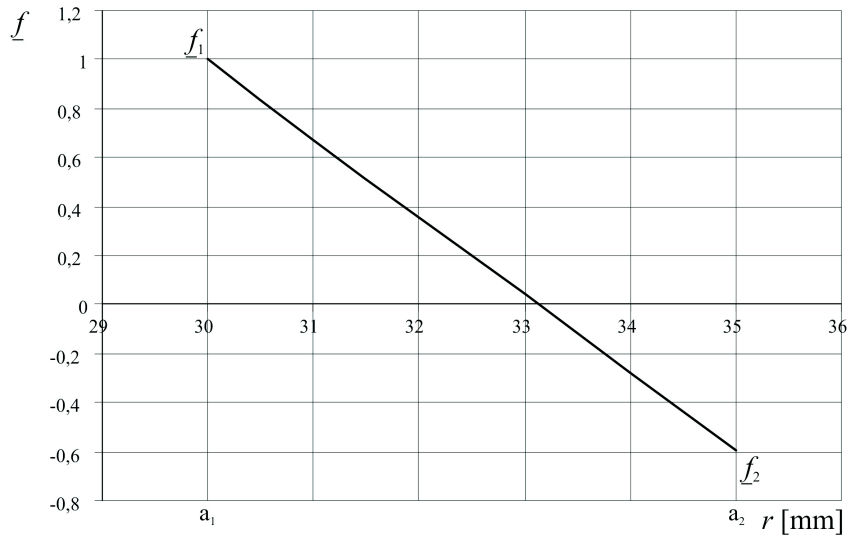

Fig. 5. Distribution of Lorentz forces along the radius in the single-coil compressing inductor of small thickness

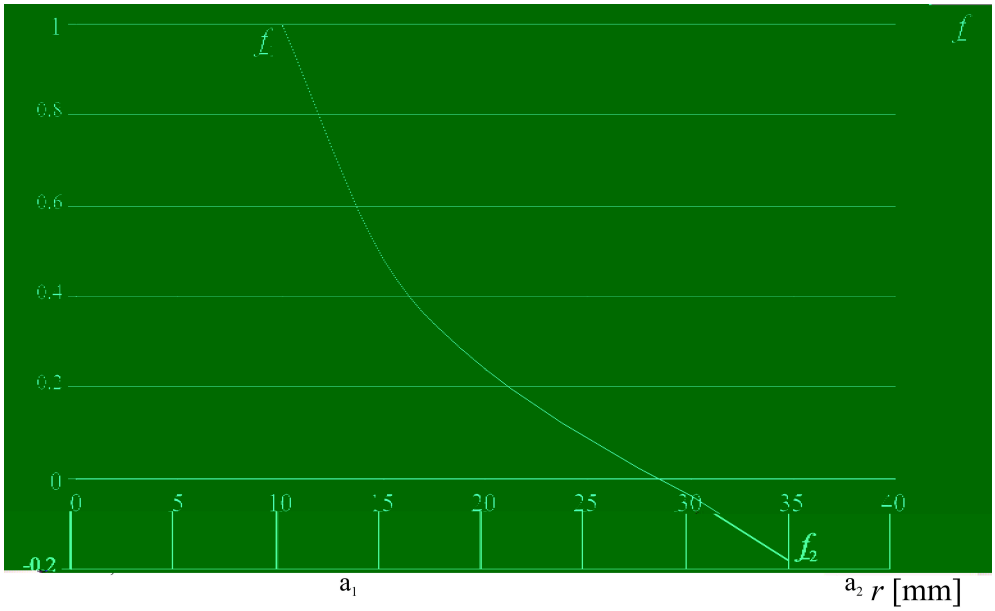

Fig. 6. Distribution of Lorentz forces in Bitter disk taking into account conductor skin effect

and then in Bitter disk, where the skin effect was taken into account. The depicted functions apply to the case when there is no pipe subjected to calibration in the inductor working zone. Diagrams in Figs. 5 and 6 show the values f_1 and f_2 of forces acting upon coil molecules on its inner and

outer surface, (Fig. 7). The senses of these forces are opposite, and their values satisfy the following condition:

$$f_1 > f_2 \tag{16}$$

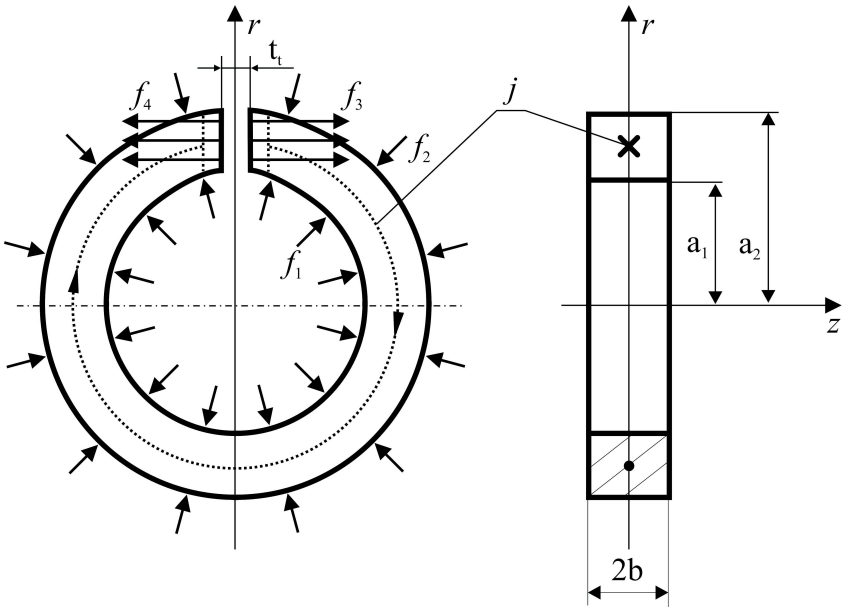

Fig. 7. Physical model of single-coil inductor loaded by Lorentz forces acting on coil delimiting surfaces

Moreover, Fig 7 shows the determined forces f_3 and f_4 of opposite senses, acting on coil ends. Their values satisfy the following condition:

$$f_3 = f_4 \tag{17}$$

The performed computations prove that the nature of distributions of Lorentz forces acting on inductor coil molecules when the calibrated pipe is present, is much the same as in Figs. 5 and 6, whereas their values change considerably. We observe magnetic field concentration within the inductor-pipe area in the following available variants of the inductor-pipe arrangement:

a. coil slid over the pipe – compressing inductor,

b. coil slid into the pipe – expanding inductor.

In the case of compressing inductor, this effect leads to the increase of force f_1 in relation to force f_2 without changing their signs (+/−). Then, the relations between values of forces may be defined by the inequality $f_1 >> f_2$. In the case of expanding inductor, the field concentration effect results in

increasing value of force f_2, and then the relation between force values is $f_2 > f_1$.

4. Strength analysis of single-coil inductors

With regard to strength, a single-coil inductor corresponds to a curved bar. The already discussed external forces acting on it can be substituted in the selected cross-section by three internal parameters – bending moment and forces: normal to the cross-section of the coil, and the tangent one, lying in the plane of this cross-section, oriented along the inductor radius. External forces acting on a single-coil inductor induce stresses in coil cross-section, which compensate these forces. When designing the inductor it is advisable to determine a cross-section in the coil, in which stresses have highest values, and which is exposed to deformation first.

For evaluation of the inductor rigidity it is also meaningful to know displacements, since from the electrodynamic technology point of view repeatability of successive processing operations is possible when specific geometry of the inductor is preserved, which means that the coil does not change its shape during semi-products processing.

Later in this article, we will present the computed distributions of reduced stress and displacement present in the single-coil inductor, obtained by analyzing only those states, in which stress and deformation components are proportional, according to the relations resulting from Hooke's law. The computations were performed using the finite elements method, by means of professional NASAN computer software. The FEMAP application was used when entering data and deriving final results. In order to make the comparative evaluation easier, computations were performed for inductors of the same length, made of the same material, and conducting current of the same intensity. The following input data were used in numerical computations of individual inductor heads: simplified continuous physical model of the analysed inductor and its overall dimensions; material constants for head components, assumed to be isotropic bodies; locations of support points. The computations were performed for the case of external load by Lorentz forces applied to the inductor, determined according to the algorithm presented in section 3. Maximum value of Lorentz forces observed during the working process was taken into account. Due to symmetry of inductor head with respect to to the plane passing through axes r, z; (Fig. 4), we performed computations only for a half of the coil, taking as boundary condition zero displacement of its points belonging to this plane. In the computations, digitising of continuous models was automatic; finite elements generated in the application were connected with each other in several points, in which con-

ditions for continuity of displacements and stresses were satisfied. External loads were replaced with forces concentrated in nodes, which resulted from continuous distributions of Lorentz forces.

4.1. Compressing inductors

Two design versions of compressing inductors were analyzed: without housing, Fig. 4 and with external jacket, Fig. 8. In the first version, different values of coil thickness g were analyzed, in the second version the analysis was carried out taking into account different values of jacket thickness $g_o = R_p - a_2$.

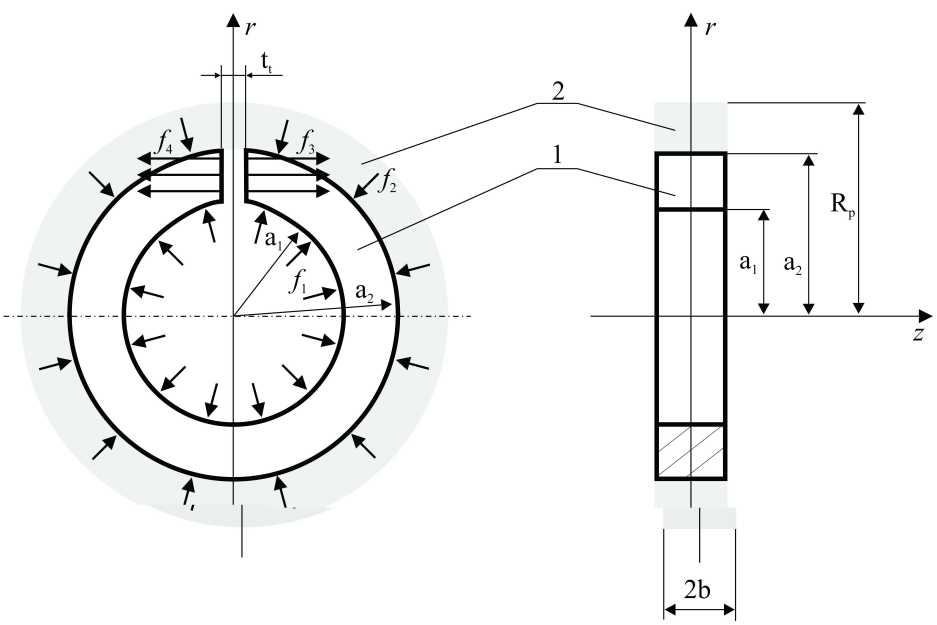

Fig. 8. Physical model of head of single-coil inductor – 1 with external jacket – 2

Numerical calculations were performed for the models presented in Figures 9 and 10, which were used to substitute continuous models from Figures 4 and 8. In the performed computations, the authors considered external forces loading the coil, obtained from continuous radial distributions of Lorentz forces determined for thin coil and Bitter coil, in which the skin effect was taken into account.

Figures 11 and 12 represent calculated numerically distributions of reduced stress and displacement produced in compressing inductor coils of different thicknesses. Due to symmetry of the coil, the distributions are shown for a half of the inductor. By analysis of the charts presented in the drawings, one can notice that regardless of the coil thickness, maximum

stresses are generated in the area on the opposite side of the structural gap t, (Fig. 4), mainly in its upper layer located by inner surface of the coil with radius a_1. Extreme values of the generated stresses are significantly smaller in the thicker coil. Under the influence of Lorentz forces, the inductor coil tends to straighten up, and its ends located along of the gap t are subject to greatest displacements. The comparison of charts in Figures 11 and 12 shows that both extreme values of generated stress and displacement are definitely smaller in the inductors made from a thick conductor. Therefore, the application of inductors made in a form of Bitter disks in compression operations is beneficial as far as strength is concerned, and for the increase of efficiency of the electrodynamic processing. However, the main disadvantage of this solution are large overall dimensions of the inductor heads, in which, for considerable reduction of potential stress and deformation, the outer diameters should be at least several times larger than the diameters of the processed pipes.

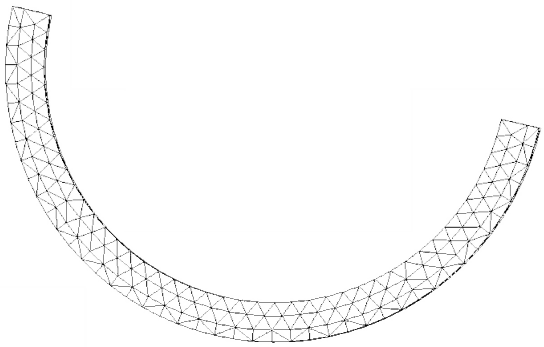

Fig. 9. Discrete model of coil inductor of small thickness drawn for numerical calculations

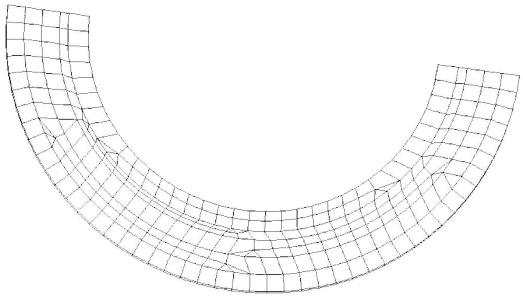

Fig. 10. Discrete model of single-coil inductor with external jacket

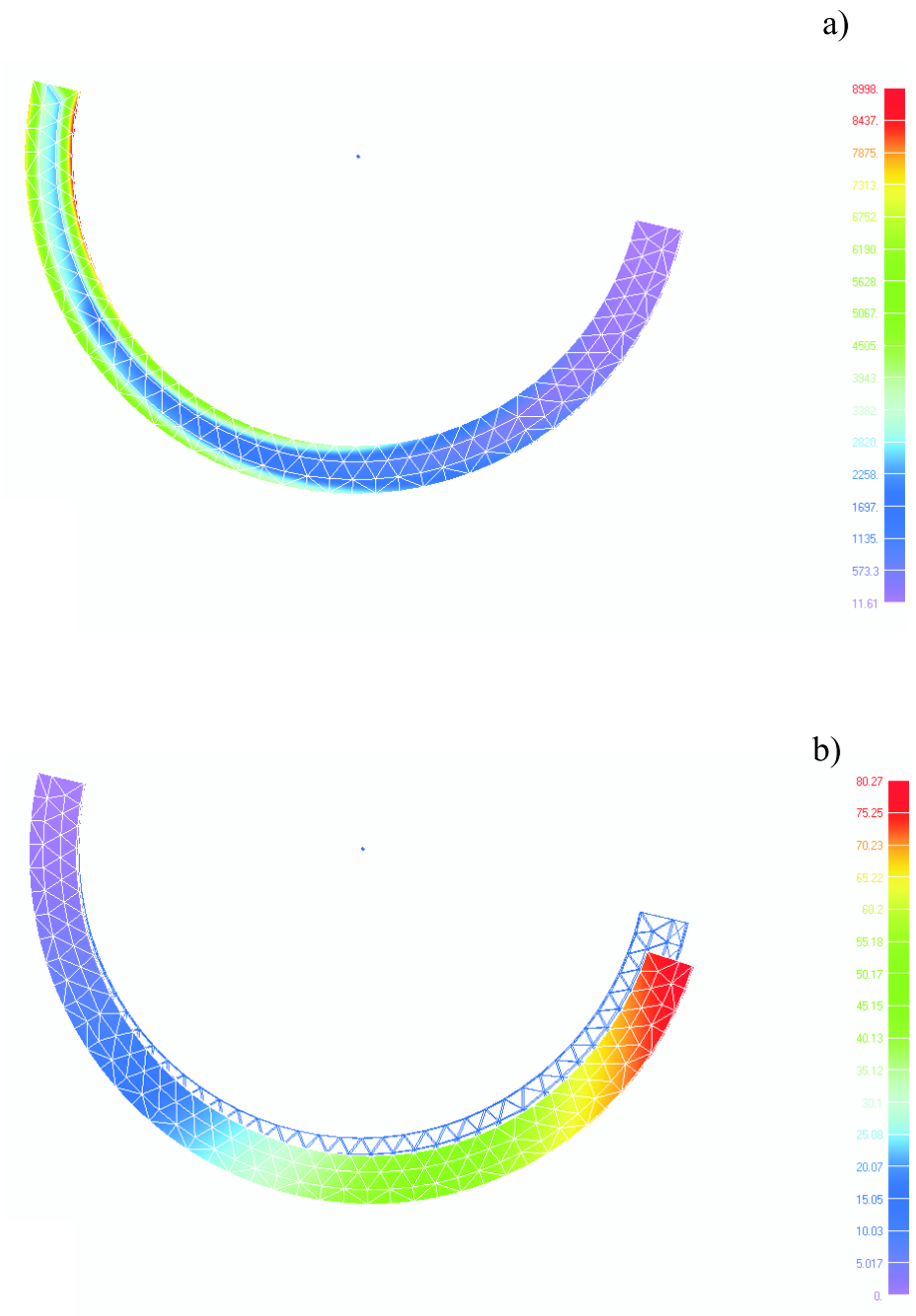

Fig. 11. Calculated numerical distributions of reduced stress – (a), expressed in MPa, and displacement – (b), expressed in mm in the inductor coil with thickness g = 5 mm

a)

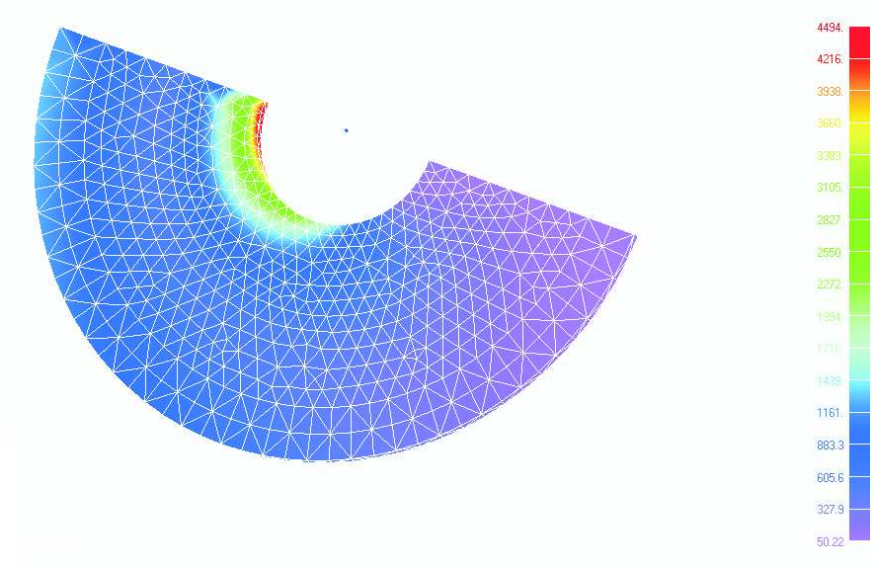

b)

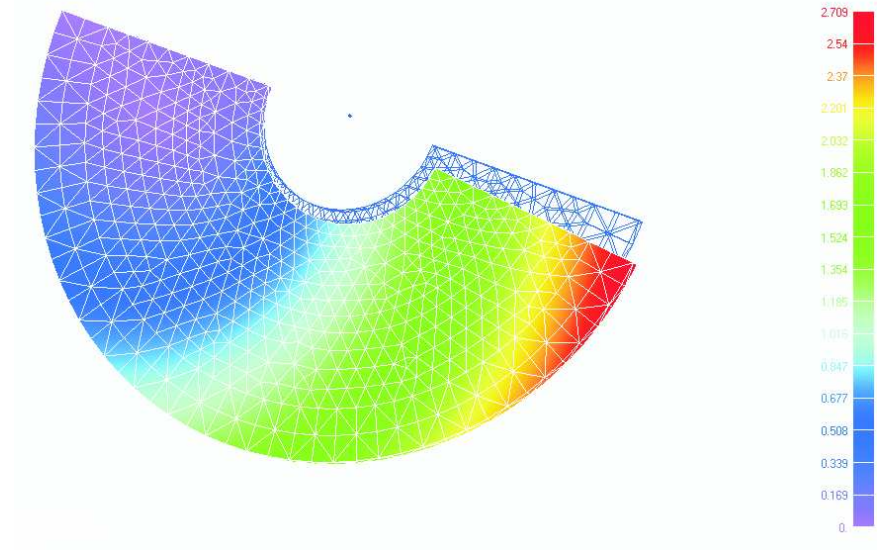

Fig. 12. Distributions of parameters as in Fig. 11: (a) – stress, (b) – displacement in inductor coil of thickness $g = 25$ mm

a)

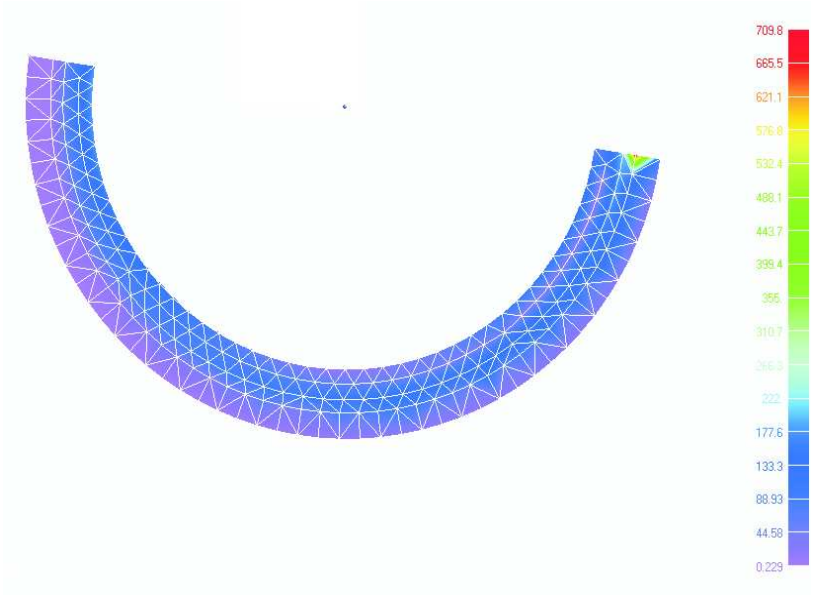

b)

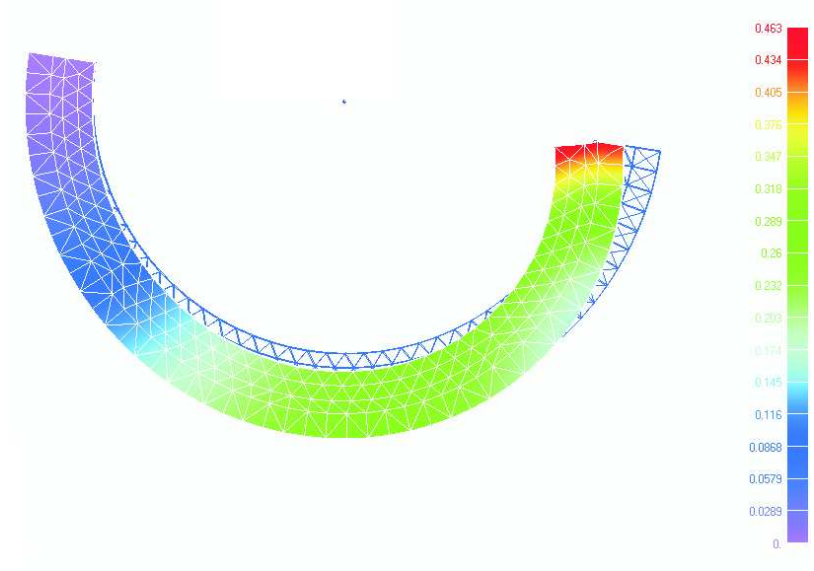

Fig. 13. Distributions of parameters as in Fig. 11 in inductor head with coil of thickness $g = 5$ mm reinforced with steel jacket of 3 mm thickness

a)

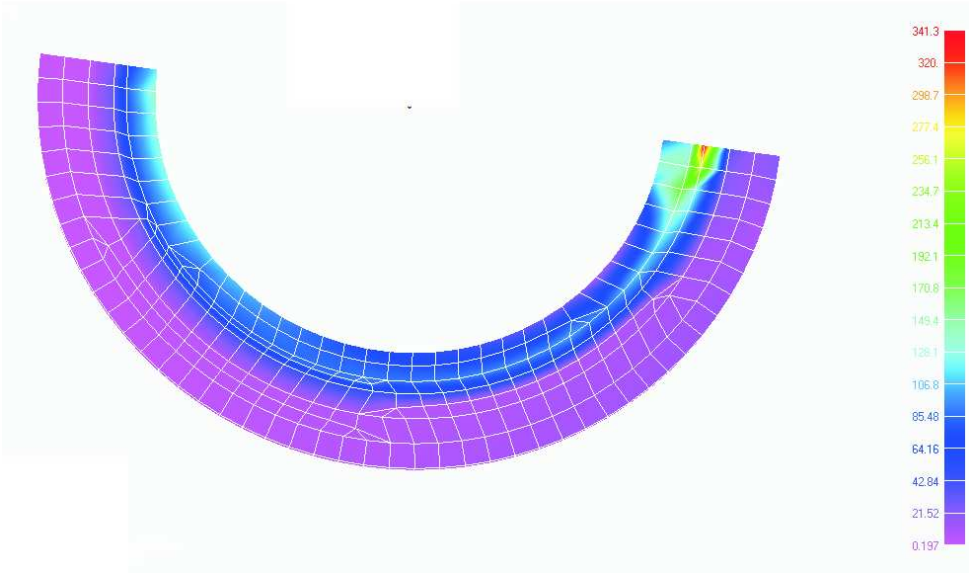

b)

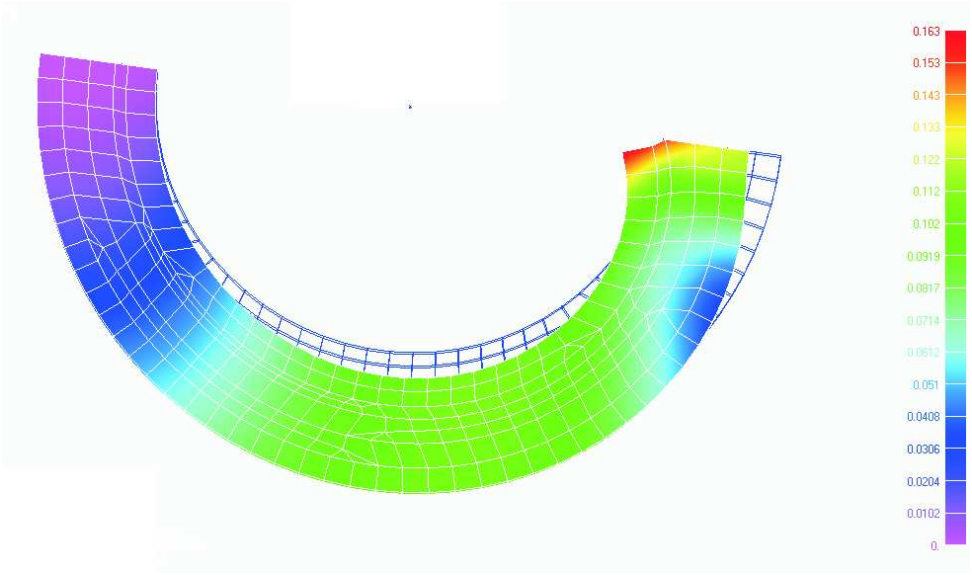

Fig. 14. Distributions for head as in Fig. 13 reinforced with jacket of 9 mm thickness

Figures 13 and 14 represent stress and displacement distributions in the inductor with external housing, with different thickness of steel jacket. Comparison of charts in Figures 11 and 13 allows us to assess advantages resulting from the use of external inductor housing. These include: no areas with local stress concentrations in the coil, and smaller maximum values of stresses by at least one order of magnitude compared to those of inductor without the housing. Furthermore, unfolding the end parts of the coil can be avoided. A disadvantageous effect of the inductor external housing, as it can be seen in the drawings, is associated with stress concentration in the contact area of the coil end and the insulation casing, which could be damaged first because its strength is lower than the strength of the jacket. The values of the mentioned stress are several times smaller than the values of maximum stress present in thin-coil jacketless inductors, and decrease significantly already with minor increase in thickness of the metal jacket, (Figures 13, 14). The presented considerations lead to an important conclusion that incorporating the external jacket allows constructing inductors using thin conductor, with high strength and reduced size.

4.2. Expanding inductors

The analysis was performed for two design versions of the inductor: coreless, (Fig. 4) and with internal non-metallic core, (Fig. 15). Numerical calculations for the coreless design were performed based on the model shown in Figure 9, by digitizing the continuous physical model, (Fig. 4). In calculations of the core head, the continuous model of the inductor (Fig. 15) was replaced by the discrete model shown in Figure 16. In the discussed expanding inductor models, the concentrated forces were determined based on the compiled continuous distribution of Lorentz forces along the coil thickness, by making use of the following relations between the values of the coil loading forces:

$$f_2 > f_1, \tag{18}$$

$$f_3 = f_4 = f_1 \tag{19}$$

Distributions of stress and displacement values obtained for the coreless inductor are shown in Figure 17, and for the core version – in Figure 18. The charts indicate that in the part of the coreless inductor located on the opposite side of its leads, in the internal part of the coil there is an area of stress with the highest values. The extreme parts of the expanding inductor are deformed most, and unlike to what takes place in the compressing inductor, the coil tends to self-clench, and the deformed coil extreme parts come close to each

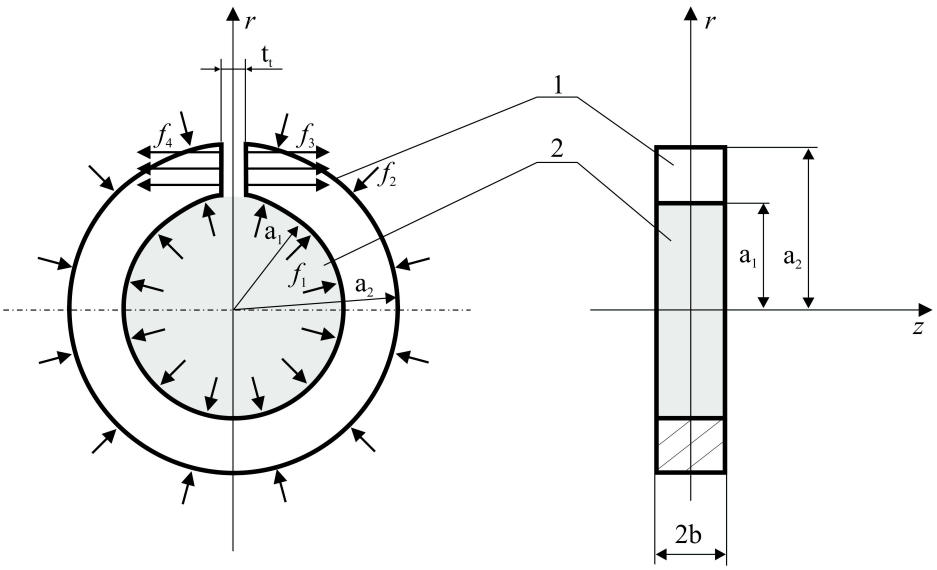

Fig. 15. Physical model of single-coil expanding inductor with internal core

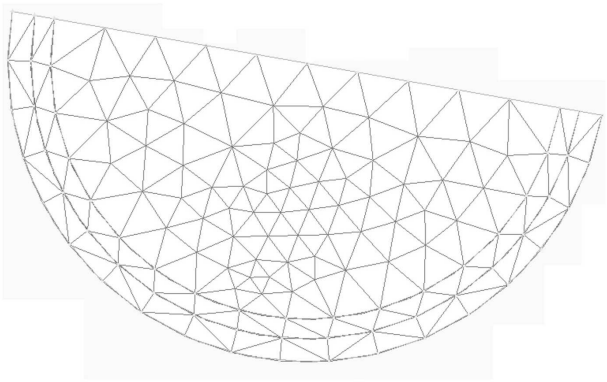

Fig. 16. Discrete model of inductor from Figure 15

other. The analysis of the charts compiled for the core inductor allows us to draw the conclusion that the use of core ensures the desired, uniform stress distribution in the coil volume, and the stress values are several dozen times smaller than in the coreless case Concentric movement of the coil towards its centre is more advantageous in the head with a core, than in a coreless inductor, for which asymmetric deformation of the coil against axis r of the inductor can be observed. For the discussed inductor, the values of displacement of the core-embedded coil are lower by some orders of magnitude than those in coreless version. However, the disadvantage of core application is the development of local stress concentrations on the outer surface of the core and the inner surface of the coil, which appear in the area

of structural gap t, with the maximum value of this stress being definitely lower than maximum values of stress present in the coreless inductor. The presented considerations show that the use of core significantly improves functional qualities of the expanding inductor, as far as strength is concerned.

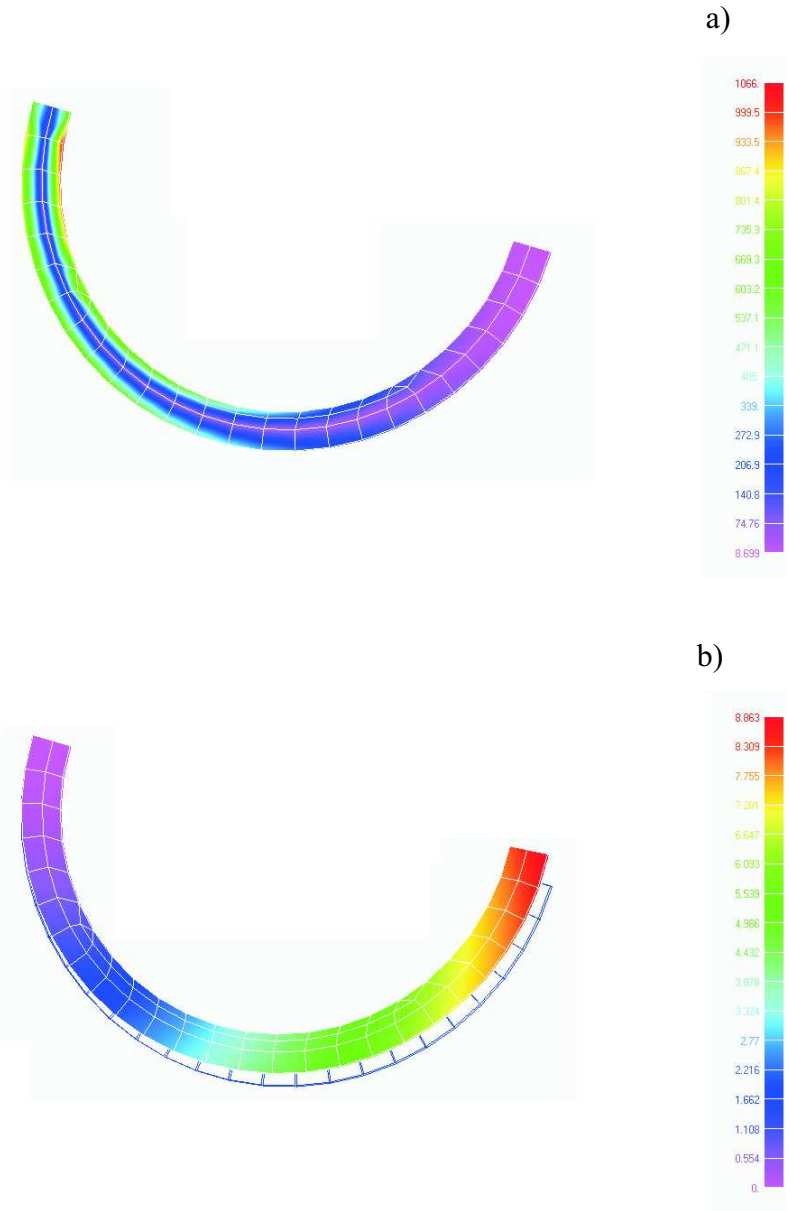

Fig. 17. Distributions of parameters as in Fig. 11 in expanding inductor without internal core

a)

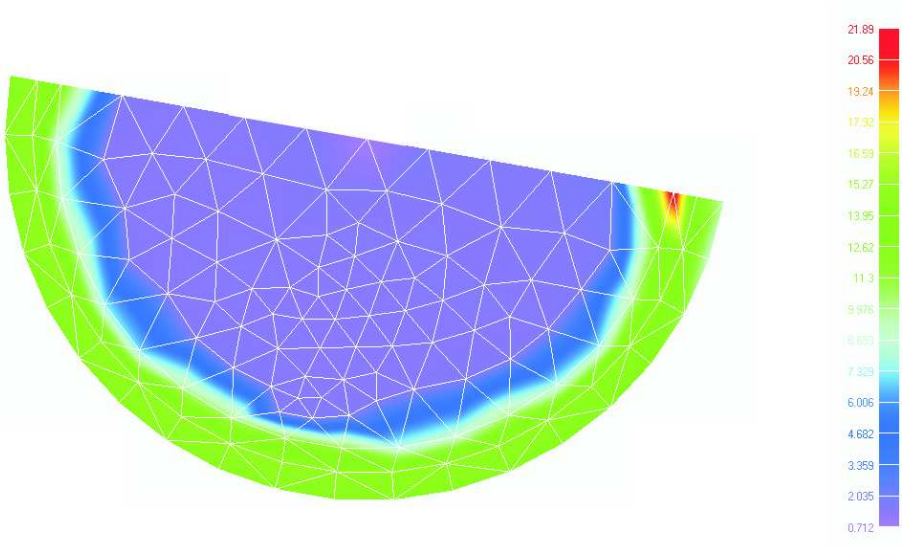

b)

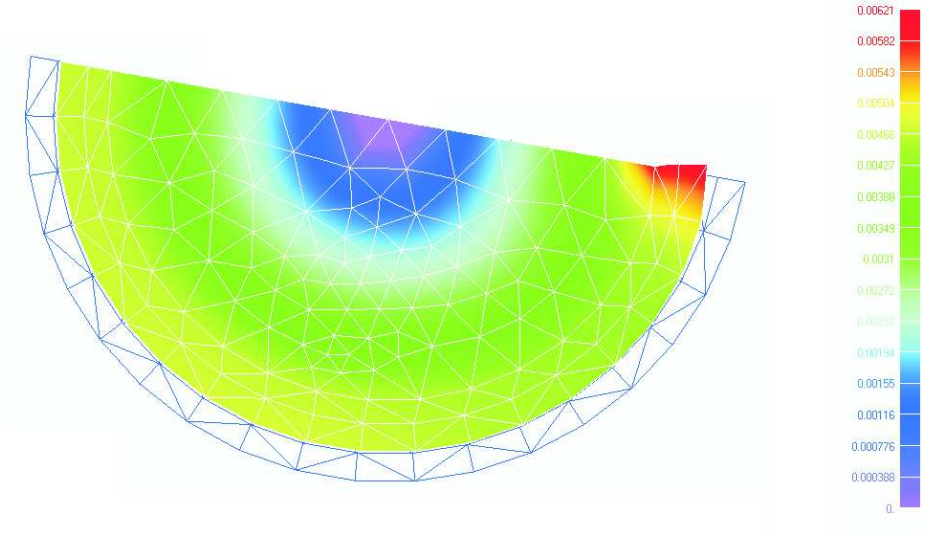

Fig. 18. Distributions of parameters as in Fig. 11 in inductor with internal non-metallic core

5. Experimental tests of Lorentz force effects

Experimental tests were designed as a type of practical verification tests, intended to assess validity of the results of the presented inductor strength

analysis. The tests were performed using sets of simple inductors made as single coils, which were connected to the output terminals of the generator used as a power source. After setting up proper high energy of the generator, the Lorentz forces generated in the inductor induced plastic strain of coils. By assuming that coil deformation appears in its part located within the maximum stress zone, a practical way of identifying this zone was determined, making comparison with the results obtained analytically possible.

The experiments were conducted for two variants of inductors made from copper wire with different thickness g: C_z – thinner coil, G_z – thicker coil.

Effects of plastic deformation of coil caused by Lorentz force generated for constant energy of the generator were evaluated for the following cases: no pipe – BR; pipe compression – SR; pipe expansion – RR. Dimensions of tested inductors are given below, (Fig. 4):

$$C_z \;-\; a_1 = 20 \text{ mm},\; a_2 = 23 \text{ mm},\; 2b = 4 \text{ mm},\; t = 3 \text{ mm}$$
$$G_z \;-\; a_1 = 2 \text{ mm},\; a_2 = 32 \text{ mm},\; 2b = 3 \text{ mm},\; t = 2 \text{ mm}$$

Pictures in drawings 19 and 20 show inductors C_z and G_z before tests (a) and the degree of deformation of their coils for: BR – (b), SR – (c). The performed tests with the inductor of small coil thickness for BR and SR cases reveal that bending of inductor ends is more intensive in the presence of the compressed pipe; then the whole coil tends to straighten up, and the coil halves, symmetrical with respect to r, (Fig. 4), displace in the coil winding plane. In the case of inductor made from thicker conductor the coil deforms similarly as in the thin-coil inductor for BR and RR cases. However, the values of displacements produced by using the same energy of generator are much smaller.

Similar experiments were conducted for a single-coil expanding inductors RR. The shapes of the inductor coils C_z and G_z after expansion tests are shown in Figure 21. During the process of pipe expansion, the inductor ends were displaced towards the center of the inductor, As it can be seen in the picture, the inductor coil halves symmetrical with respect to axis r of the inductor were turned around this axis assuming orientation in the plane non-parallel to the coil winding plane. This effect indicates that the coil lost its stability under the generated stress.

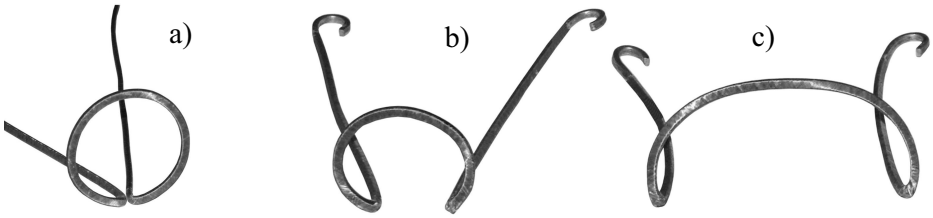

Fig. 19. Deformation of inductor coil made from thin conductor

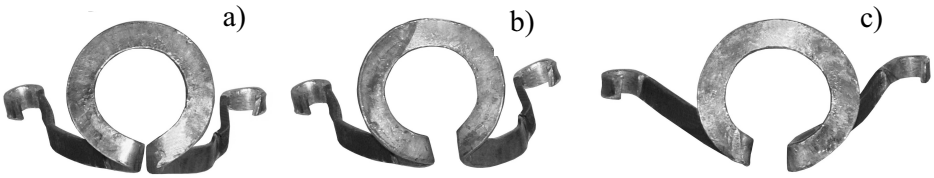

Fig. 20. Deformation of coil inductor made from thicker conductor

Fig. 21. Deformation of coil in compressing inductor

6. Summary

Application of the new, unconventional technologies developed at research centers, such as electrodynamic processing of metals requires solving numerous problems regarding construction of appropriate instruments. The

article presents results of the tests conducted at the AGH-University of Science and Technology, the purpose of which was to identify strength problems essential when designing fixed inductors used as tools in the said technology. The material presented in the article includes a description of different design variants of single-coil inductors intended for compression and expansion of pipes. The author demonstrated that increased coil thickness and the presence of external housing have a positive effect on strength of compressing inductors. Advantages of the internal core reinforcing the inductor head structure, which are important for strength, were exposed in expanding inductors.

Manuscript received by Editorial Board, June 15, 2005;
final version, November 28, 2005.

REFERENCES

[1] Bednarczyk J.: Distributions of forces in the inductors used in metal processing in pulse magnetic field. Journal of Materials Processing Technology, 2003, Vol. 133, pp. 340÷347.
[2] Bednarczyk J.: Plastyczna obróbka metali metodą elektrodynamiczną. Kraków, FSI, 2002.
[3] Bednarczyk J.: Distribution of forces in inductors for electrodynamic working of metals. The Archive of Mechanical Engineering, 1995, Vol. XLII, Book 3–4, pp. 233÷250.
[4] Bednarek S.: Konstrukcja cewki do nieniszczącego wytwarzania silnych impulsowych pól magnetycznych. Przegląd Elektrotechniczny, 2001, nr 1, str. 13÷16.
[5] Bendjima B., Srairi K., Féliachi K.: A cuopling model for analysing dynamical behaviours of an electromagnetic forming system. IEEE Transactions on Magnetics, Vol. 33, No. 2, pp. 1638÷1641.
[6] Dyląg Z., Jakubowicz A., Orłoś Z.: Wytrzymałość materiałów. Warszawa, WNT, 1997.
[7] El-Azab A., Garnich M., Kapoor A.: Modeling of the electromagnetic forming of sheet metals: state-of-the-art future needs. Journal of Materials Processing Technology, 2003, Vol. 142, pp. 744÷754.
[8] Fenton G. K., Daehn G. S.: Modeling of electromagnetically formed sheet metal. Journal of Materials Processing Technology, 1998, Vol. 75, pp. 6÷16.
[9] Frings P. H., Oudendijk M. G. N., Gersdorf R., Van Schalkwijk R.: The mechanical design of coils for generating high magnetic field. IEEE Transactions on Magnetics, 1994,Vol. 30, No. 4, pp. 2168÷2171.
[10] Głuch G.: Badania nad trwałością induktorowych narzędzi stosowanych w elektrodynamicznej obróbce metali. Doctor's thesis AGH Krakow, 2005.
[11] Knoepfel H.: Magnetic fields: a comprehensive theoretical treatise for practical use. New York, John Wiley&Sons, 2000.
[12] Kruszewski J.: Metoda elementów skończonych w dynamice konstrukcji. Warszawa, Arkady, 1984.
[13] Kucharov W. D., Proskurjakov N. E., Pasko A. N.: Koniečnoelementnyje varianty vyčislenia deformacji w zadačach magnitno-impulsnoj štampovki. Kuzniečno Štampovočnoje Proizvodstwo, 1998, No. 10, pp. 16÷17.
[14] Rusinov A. I.: High precision computation of Solenoid Magnetic Fields by Garret's methods. IEEE Transactions on Magnetics, 1994, Vol. 30, No. 4, pp. 2685÷2688.
[15] Soung Ho Lee, Dong Nyung Lee: A finite element analysis of electromagnetic forming for tube expansion. Journal of Engineering Materials and Technology, 1994, Vol. 116, pp. 250÷254.

[16] Unger J., Stiemer M., Svendsen B, Blum H.: Multifield modeling of electromagnetic metal forming processes. Journal of Materials Processing Technology, 2006, Vol. 177, pp. 270÷273.
[17] Van Bockstal L., Herlach F., Askenazy S.: Analitical expression for the optimized radial distribution of internal reinforcement in high magnetic coils. IEEE Transactions on Magnetics, 1994,Vol. 30, No. 4, pp. 2176÷2179.

Stany naprężeń i odkształceń w jednozwojowych induktorach stosowanych do kalibracji rur metodą elektrodynamiczną

S t r e s z c z e n i e

W artykule przedstawiono wyniki badań realizowanych w Akademii Górniczo-Hutniczej w Krakowie dotyczących wytrzymałości jednozwojowych induktorów stanowiących narzędzia w elektrodynamicznej obróbce rur. Omówiono charakter objętościowych sił Lorentza działających w jednozwojowych induktorach ściskających i rozpęczających, a także zaprezentowano wyznaczone numerycznie rozkłady naprężeń i przemieszczeń powstających w zwojach pod wpływem tych sił. Zagadnienia rozważane w artykule są istotne przy projektowaniu trwałych induktorów przeznaczonych do celów przemysłowych.